# Reconstruction of mass balance and firn stratigraphy during the 1996-2011 warm period at high-altitude on Mt. Ortles, Eastern Alps: a comparison of modelled and ice core results

Luca Carturan[1], Alexander C. Ihle[2,3], Federico Cazorzi[4], Tiziana Lazzarina Zendrini[1], Fabrizio De Blasi[1,5], Giancarlo Dalla Fontana[1], Giuliano Dreossi[6], Daniela Festi[7], Bryan Mark[3], Klaus Dieter Oeggl[8], Roberto Seppi[9], Barbara Stenni[6], Paolo Gabrielli[10]

[1]Department of Land, Environment, Agriculture and Forestry, University of Padua, Legnaro, Italy

[2]Department of Earth and Environmental Sciences, University of Rochester, Rochester, USA

[3]Department of Geography and Byrd Polar and Climate Research Institute, Ohio State University, Columbus, USA

[4]Department of Agricultural, Food, Environmental and Animal Sciences, University of Udine, Udine, Italy

[5]Consiglio Nazionale delle Ricerche - Istituto di Scienze Polari, c/o Ca' Foscari University of Venice, Venice, Italy

[6]Department of Environmental Sciences, Informatics and Statistics, Ca' Foscari University of Venice, Venice, Italy

[7]GeoSphere Austria, Department of Geoanalytics and Reference Collections, Vienna, Austria

[8]Department of Botany, University of Innsbruck, Innsbruck, Austria

[9]Department of Earth and Environmental Sciences, Pavia, Italy

[10]Italian Glaciological Committee, Torino, Italy

*Correspondence to:* Luca Carturan (luca.carturan@unipd.it)

**Abstract**

Paleoclimatic glacial archives in low-latitude mountain regions are increasingly affected by melt, which leads to heavy percolation and can remove snow and firn accumulated across months, seasons or even years. Proxy system models, used for improved interpretation of glacial proxies and paleoclimatic reconstructions, generally do not account for melt because they are optimized for sites where snow layer removal by melting is negligible. In this paper, we present a mass balance model applied to the Mt. Ortles drilling site, at 3859 m a.s.l. in the Eastern Italian Alps, with the aim of building a pseudo proxy of atmospheric conditions during the formation of snow layers survived to ablation. This pseudo proxy is useful for improved dating and environmental interpretation of firn layers (<15 m depth), affected by significant melt in the period 1996-2011, which includes the extremely warm summer 2003. Here we show that the model significantly improves

the interpretation of the firn stratigraphy. This is fundamental for detecting melted layers and for refining the dating of the core based on traditional annual layer counting of stable isotope and pollen seasonal oscillations.

## 1 Introduction

Atmospheric warming is threatening paleoclimatic glacial archives, particularly those located in low-latitude mountain areas (e.g. Gabrielli et al., 2010; Huber et al., 2024). When compared to polar ice sheets in Greenland and Antarctica, these glaciers are now altitudinally closer to their lower limits of formation and preservation.

Long before their complete disappearance, glacial archives are affected by post-depositional processes caused by increasing temperature, which modifies and ultimately overprints their paleoclimatic signals. Increasing frequency and intensity of surface melt events lead to snow/firn layer mass loss and heavy percolation of meltwater through the firn. This obliterates part of the glacial archive and smooths or dislocates intra/inter-annual variations of chemical impurities of interest for paleoclimatic reconstructions (Dietermann & Weiller, 2013; Gabrielli et al., 2010; Hashimoto et al., 2005; Lee, 2014; Moran et al., 2011; Moser et al., 2024, Thompson et a., 2011, 2021; Unnikrishna et al., 2002).

It is unclear how extreme melt events, such as the summer 2003 heat wave in the European Alps (Zappa and Kan, 2007; García-Herrera et al., 2010), affect the preservation of ice core archives. This kind of events may significantly change the original isotopic record, melting the snow accumulated over several months or years (Gabrielli et al. 2010). In addition it is unknown whether such extreme events may relocate less mobile impurities such as pollens or black carbon, as their annual cycle is generally preserved under melting conditions, and are therefore used for ice core dating (Pavlova et al., 2015; Festi et al., 2021; Takeuchi et al., 2019; Moser et al., 2024).

Atmospheric warming also affects snow water content and its metamorphism, which control snow redistribution by wind. For this reason, snow drifting is expected to be most effective for cold and dry snow and less so for wet snow and melt-freeze crusts (Haeberli and Alean, 1985, Li and Pomeroy, 1997; He and Ohara, 2017). This process can influence the snow accumulation rate and the formation/preservation of the isotopic record and other chemical signals (Bohleber, 2019; Bohleber et al., 2013; Nakazawa et al., 2005). This adds complexity to dating and interpretation of ice cores archives, particularly for those retrieved at high elevation in non-polar glacierized areas subjected to significant snow melt and wind redistribution. In this case, annual layer counting is difficult because surface melt and/or wind redistribution remove snow layers formed across months or seasons (Neff et al., 2012). As these processes are typical of these mid-to-low latitude regions and are part of the glacial archive's response to climate change, their understanding is a fundamental prerequisite for paleoclimatic reconstructions.

Glacier mass balance modelling at ice core drilling sites is useful to reconstruct the formation and preservation of glacial archives and their ongoing changes due to atmospheric warming. Mass balance models can provide information on the amount of surface melt, meltwater percolation, and magnitude of snow accumulation by precipitation and wind drifting. Overall, these model outputs can help to detect and characterize events linked to i) snow layer formation, ii) snow layer removal, and iii) snow layer modifications (e.g. warming, wetting, refreezing). This information may also help in detecting deviations of ice core proxies from the generally assumed linear, univariate recording of local temperature (Evans et al., 2013). In fact, this assumption may not hold in the long term, particularly under extreme conditions such as current or past warm climatic phases, especially at sensitive locations such as mid-to-low-latitude glacierized areas.

Proxy system models (models that describe the processes by which environmental conditions are recorded in a proxy archive) linked to isotope-enabled atmospheric general circulation models (models that describe isotopic variations in precipitation for a geographic area) are increasingly used to constrain ice core-based paleoclimatic reconstructions and for complementing interpretations based solely on statistical analyses (Evans et al., 2013). Proxy system models of various complexities were developed for ice core proxy interpretation (e.g., Brönnimann et al., 2013; Hurley et al., 2016; Okazaki and Yoshimura, 2019). These models reconstruct how stable water isotopes are recorded in ice core archives, generating a pseudo proxy that is compared to the actual proxy, to complement it and improve its paleoclimatic interpretation. For example, the possibility to disentangle different processes (temperature, intermittency of precipitation, diffusion) affecting the isotopic records to extract the "real" climatic signal, by using a so called "virtual" ice core, has been studied for Antarctica (Laepple et al, 2018).

These models are optimized for sites where snow layer removal by melting is negligible and snow redistribution can be accounted for by stacking ice core records from adjacent sites located in the same area (e.g., Ekaykin and Lipenkov, 2009). Additionally, models implicitly assume stationarity (or negligible variations) of snow redistribution, melt, and meltwater percolation. This is not always the case, particularly for low-latitude drilling sites where cold climatic phases that are favourable for ice core proxy formation and preservation alternate with warm climatic phases that are unfavourable.

The Mt. Ortles drilling site, at 3859 m a.s.l. in the Eastern Alps (Italy), has been characterised by a rapid warming of the firn and snow layers since the 1980s. Atmospheric warming is seriously threatening this paleoclimatic archive (Gabrielli et al., 2010) due to the increasing length and intensity of the ablation season, causing significant surface melt and meltwater percolation. In summer the firn layer is now entirely isothermal at the pressure melting point (Carturan et al., 2023). The ice below the firn-ice transition (30 m depth) is still cold, with temperature down to -2.8°C close to the bedrock in 2011 (Gabrielli et al., 2012). This shows that conditions favourable for glacial archive formation and preservation still exist on Mt. Ortles. However, the relatively low elevation of this ice core-drilling site makes it sensitive to climatic fluctuations and particularly vulnerable to non-linear processes controlled by snowmelt, snow metamorphism, and wind redistribution.

In this paper, we present a model-based reconstruction of the mass balance history and firn stratigraphy at the Mt. Ortles drilling site in the 1996-2011 warm period, including the extremely warm summer 2003 (García-Herrera et al., 2010). The aim is understanding the effects of exceptionally warm periods on glacier mass balance and the ice core paleoclimatic archive. Specifically, the mass balance model used in this work was implemented to: i) model the formation of snow and firn layers, ii) identify snow layers removed by ablation, iii) reconstruct the air temperature during the formation of snow layers that survived successive ablation. This latter is a pseudo proxy that we ultimately compare to stable water isotopes retrieved in the firn layers of the same period, to revise the dating of the firn portion of the Mt. Ortles ice core.

## 2 Study area

Mount Ortles (3905 m a.s.l.), in the Ortles-Cevedale Mountain Group, is the highest summit of South Tyrol in the Eastern European Alps. Its northern flank is covered by the Alto dell'Ortles Glacier (Oberer Ortlerferner-Vedretta Alta dell'Ortles), which extends over an area of 1.06 $km^2$ (2017) and ranges in elevation between 3018 and 3905 m a.s.l. (Fig. 1). The ice core drilling site is located at 3859 m a.s.l. in the upper accumulation area, close to a saddle (Figs. 1 and 2).

105 The glacier's maximum thickness at the drilling site is about 75 meters (Gabrielli et al., 2012) and the ice is ~7-kyr old at
106 the glacier base (Gabrielli et al., 2016). In this zone the glacier is polythermal, with temperate firn and cold ice underneath
107 the firn-ice transition, at ~30 m depth (Gabrielli et al., 2012). The Ortles ice archive is one of the only two cold ice archives
108 found in the eastern Alps, with the other being the nearby Weißseespitze (Cima del Lago Bianco) summit ice dome
109 (Bohleber et al., 2020; Gabrielli et al., 2012).

110 The local climate is characterized by a continental regime, with a mean annual precipitation in the period 1981-2010 of
111 800–950 mm $yr^{-1}$ at the valley floor in Solda (Adler, 2015). The annual precipitation on the top of Mt. Ortles is estimated
112 to range between 1300 and 1400 mm, using in-situ mass balance observations performed between 2009 and 2016,
113 (Carturan et al., 2023). This precipitation estimate is subject to large spatial variability due to the influence of wind on
114 snow accumulation and redistribution.

115 The mean annual air temperature at 3850 m a.s.l. on Mt. Ortles is about -9°C. On the glaciers of the Ortles-Cevedale
116 Group the snow cover follows a typical annual cycle, with accumulation prevailing between October and May, and
117 ablation between June and September. Due to the high elevation of the drilling site, snowfalls are also frequent during
118 summer. There is high interannual variability in the amount and duration of ablation events, which occur primarily during
119 heatwaves. Liquid precipitation is very rare, although some rain events have been recorded at the drilling site elevation
120 over the past 15 years (Carturan et al., 2023).

121

122

123

124

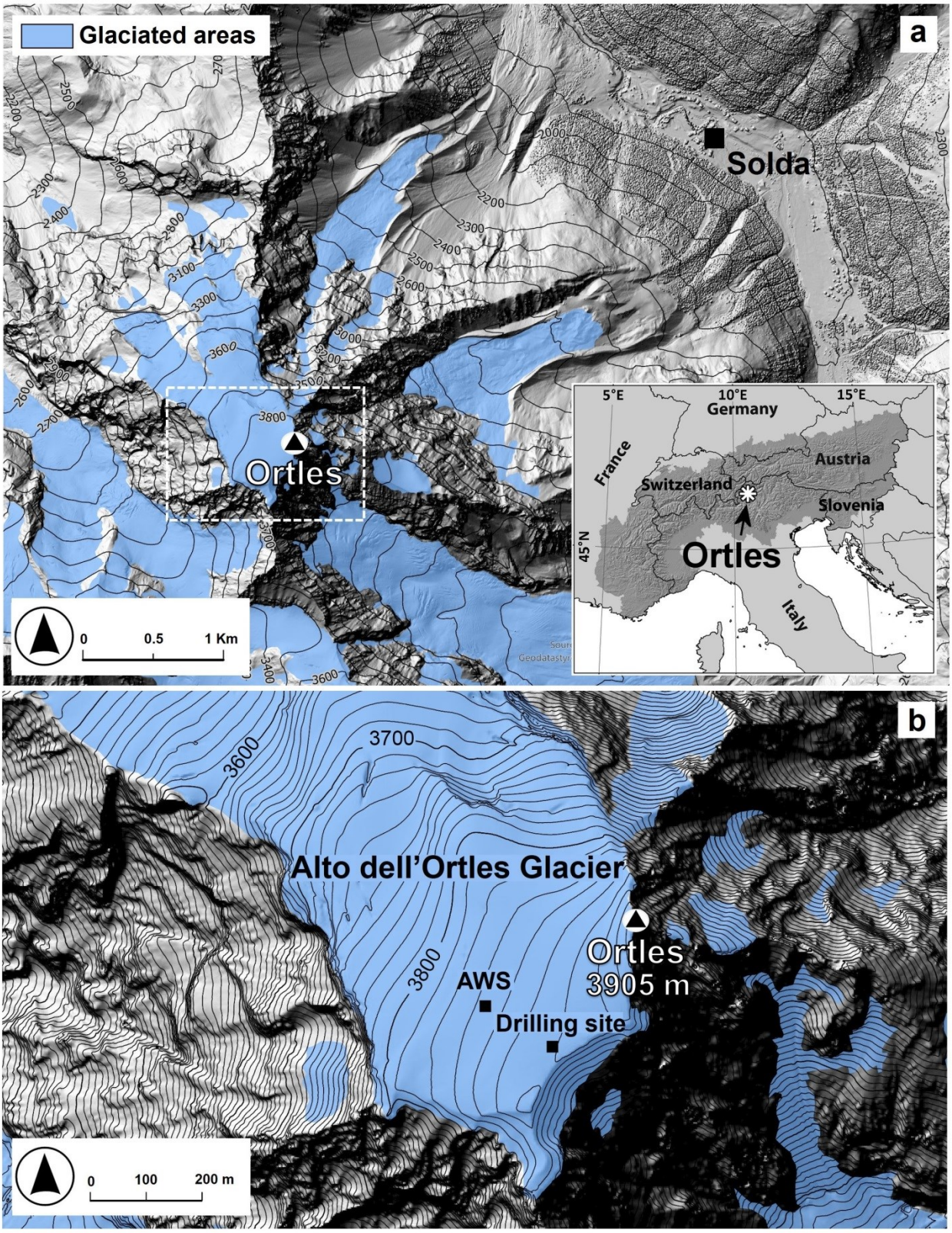


Figure 1: Location of the drilling site and automatic weather station (AWS) on Mt. Ortles. The background hill-shaded DEM (2017 lidar survey) is from http://geocatalogo.retecivica.bz.it/ (last access: 10 January 2025) (Agenzia per la Protezione civile, Autonomous Province of Bolzano).

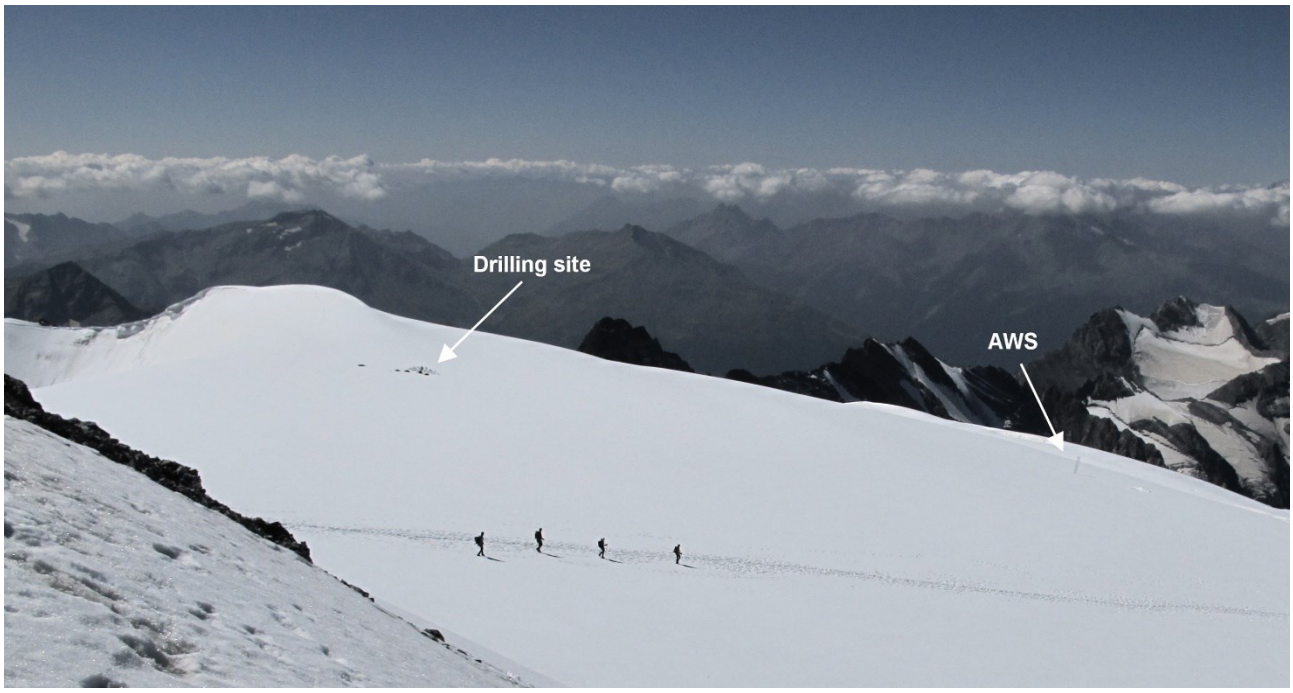


Figure 2: Photo of the upper accumulation area of Alto dell'Ortles Glacier taken from the summit of Mt. Ortles on 31 August 2015.

## 3 Methods

### 3.1 Ice core drilling operations

Four ice cores were drilled within 20 m of each other during September and October 2011 on a small col on the Alto dell'Ortles Glacier, between the summit of Mt. Ortles and the Vorgipfel (UTM zone 32T, 618364 m easting, 5151531 m northing, 3859 m altitude). In this study, we focus on core 1, which reached 73.53 m depth, because it is the only one for which both complete isotope and pollen records are available. (Gabrielli et al., 2016).

### 3.2 Ice core analyses

Ortles core 1 was cut in a cold room (-20°C) at the Ca' Foscari University of Venice (Italy). Analysis resolution increased with increasing depth, from 9 cm per sample (0-5 m depth), to 2 cm per sample (from 49 m to bottom).

Oxygen and hydrogen isotopic composition analyses were performed with two analytical methods. One method uses the well-established $CO_2$-$H_2$/water equilibration technique (Horita et al., 1989) which couples an automatic equilibration device (Finnigan MAT HDO 1086) with an isotope ratio mass spectrometer (Thermo-Fisher Delta Plus Advantage). Five ml of water were used and the analytical uncertainty for $\delta^{18}O$ and $\delta D$ was ± 0.05‰ (1σ) and ±0.7‰ (1σ), respectively. The other method was the wavelength-scanned cavity ring-down spectroscopy technique (PICARRO model L1102-i). Since the injections of water samples can be affected by between-sample memory effects (Penna et al., 2012), samples

were injected (2 µl) 8 times and results were filtered using an outlier test. The analytical uncertainty for $\delta^{18}O$ and $\delta D$ was ± 0.10‰ (1σ) and ±0.5‰ (1σ), respectively. In each analysis run, two internal standards (periodically calibrated against the IAEA international standards V-SMOW2 and SLAP2) were analysed along with the samples, and used for building a calibration curve. The results were reported in the usual delta notation (δ) and expressed as per mil (‰).

Pollen analyses were performed at the Institute of Botany of the University of Innsbruck. Aliquots of up to 35 ml water (depending on sample resolution) were used. Each sample was decontaminated with cold distilled water and the volume of the water resulting from the ice melting was measured. Samples were processed with acetolysis (Erdtman, 1960) and the pollen content was concentrated by hydro-extraction (centrifugation) and then prepared in glycerine slides (Faegri and Iversen, 1989). The complete pollen content of the samples has been identified and quantified, as detailed in Festi et al. (2015). For each sample, pollen concentration (grains $ml^{-1}$) was calculated. To detect the seasonality a principal component analysis (PCA) has been performed on the pollen dataset according to the methodology developed in Festi et al (2015). Three principal components indicative of the three main flowering seasons (spring, early summer and late summer) were hereby extracted and are presented graphically. Peaks in component score values of a specific PC reflect a pollen content characteristic predominant in the season corresponding to that particular PC. This method was applied to the dataset as previous studies showed that the Ortles glacier pollen assemblages are representative for the regional vegetation and comparable with airborne assemblages recorded at the nearby aerobiological stations (Festi et al., 2015).

### 3.3 Mass balance observations

Seasonal and annual glacier mass balances were measured at the drilling site and at the automatic weather station site (Section 3.4., Figs. 1 and 2) from June 2009 to September 2014. Winter balance observations were typically carried out in June/early July before the onset of melt, while summer/annual balance were performed in late August/early September at the end of the melt season.

Observations consisted of snow depth soundings with a metal probe in the surroundings of the two sites, and of snow/firn density measurements inside snow pits dug to the previous summer surface. Detailed snow stratigraphic observations were carried out at shaded snow pit walls, comprising snow/firn temperature, hardness, grain type and size, location of ice lenses and dust layers (e.g. Gabrielli et al. 2010). Stratigraphic observations were helpful in recognising summer surfaces both in snow pits and during snow depth soundings. Density measurements were used to convert snow depths into water equivalent depths.

### 3.4 Meteorological observations

The meteorological data used in this work are from an automatic weather station (AWS) located in the valley floor village of Solda (Fig. 1, 1907 m a.s.l.) about 4.5 km northeast of Mt. Ortles. This AWS is part of the network of AWSs operated by the Hydrological Office of the Autonomous Province of Bolzano (meteo.provincia.bz.it).

To collect additional meteorological observations, the Ortles paleoclimatological project (ortles.org) installed an AWS close to the drilling site in October 2011 (Figs. 1 and 2). The AWS worked until June 2015 and was equipped with air temperature, relative humidity, wind speed and direction, shortwave and longwave incoming and outgoing radiation, and snow depth sensors. Details on Ortles AWS instrumentation and datasets are provided in Carturan et al. (2023).

### 3.5 Mass balance modelling

The mass balance model used in this study is EISModel, an energy-index model implemented for mass balance computations on glaciers and seasonal snowpacks. The model in its original version is described by Cazorzi and Dalla Fontana (1996), followed by Carturan et al. (2012a) who presented an advanced version for glacial environments. The model was further developed for applications on Mt. Ortles, as detailed in Festi et al. (2017). In this section, we recall the main features of EISModel and describe how it was applied to the study area.

The model was applied at hourly time steps. Snow accumulation was calculated from the hourly precipitation data of the Solda AWS, validated against other neighbouring AWSs (Madriccio at 2825m and Cima Beltovo at 3328 m) and corrected for gauge under-catch errors using the method proposed by Carturan et al. (2012b). Precipitation was extrapolated to the elevation of the study site using a precipitation linear increase factor (PLIF, % $km^{-1}$), which is a lumped parameter that accounts for the vertical increase of precipitation with elevation, preferential deposition, and erosion by wind. Precipitation was classified as liquid or solid depending on the hourly air temperature, which is extrapolated from the Solda AWS using monthly-variable temperature lapse-rates calculated between the Solda and Ortles AWSs.

Hourly melt rates were calculated using the following equation:

$$MLT_t = RTMF \cdot CSR_t(1 - \alpha_t) \cdot T_t \quad (1)$$

where $RTMF$ is the radiation–temperature melt factor (mm $h^{-1}$ $°C^{-1}$ $W^{-1}$ $m^2$), $CSR_t$ (W $m^{-2}$) is the clear-sky shortwave radiation computed hourly based on the local topography, $T_t$ is the air temperature, and $\alpha_t$ is the surface albedo calculated in function of cumulative positive $T_t$ (Carturan et al., 2012a).

The RTMF and PLIF parameters were initially calibrated at the Ortles AWS site using mass balance observations carried out between 2009 and 2014. For a more robust calibration, we extended backwards to 2005 the mass balance observations, using pollen dating of firn layers (Festi et al., 2017). We preferred to initially calibrate the model at the AWS site, rather than at the drilling site, because field observations are more extensive and consistent at that site. The PLIF parameter was then recalibrated at the drilling site, to account for lower snow accumulation. Finally, the model was applied to reconstruct the cumulated mass balance in the period from September 1996 to September 2011.

The pseudo proxy to be compared to stable water isotopes in firn cores was obtained by calculating the air temperature during the formation of snow layers that survived to ablation. We define as a snow layer the water equivalent of snow that accumulates at the surface in one hour. For each snow layer surviving the following ablation, the model provided its time and date of formation and the air temperature during its deposition, which is a variable named SLFT (snow layer formation temperature). The model did not explicitly simulate the time variability of snow removal by wind drift, which was assumed to be constant in time, and was computed statistically by means of the PLIF multiplicative factor. The water equivalent thickness of each snow layer composing the final snowpack was finally adjusted to account for layer thinning with depth, using the Nye (1963) ice flow model (similarly to, for example, Eichler et al. (2000) and Brönnimann et al. (2013)).

## 4 Results

## 4.1 Model calibration

The calibrated values of the two parameters RTMF and PLIF optimized at the AWS site on Mt. Ortles were $10^{-3}$ mm $h^{-1}$ °$C^{-1}$ $W^{-1}$ $m^2$ and 15 % $km^{-1}$, respectively. At the ice core drilling site (located 200 m uphill of the AWS), the PLIF was recalibrated to 8 % $km^{-1}$ to account for lower snow accumulation, probably due to higher wind erosion.

The model performance, expressed by the root mean square error (RMSE), is better for summer balance compared to winter balance, and in closer agreement with observations at the AWS site, compared to the drilling site (Fig. 3). This behaviour was expected because the drilling site is more exposed to wind action and likely experiences stronger snow redistribution, particularly during winter. These results are similar to previous applications of EISModel on Mt. Ortles (Festi et al., 2017).

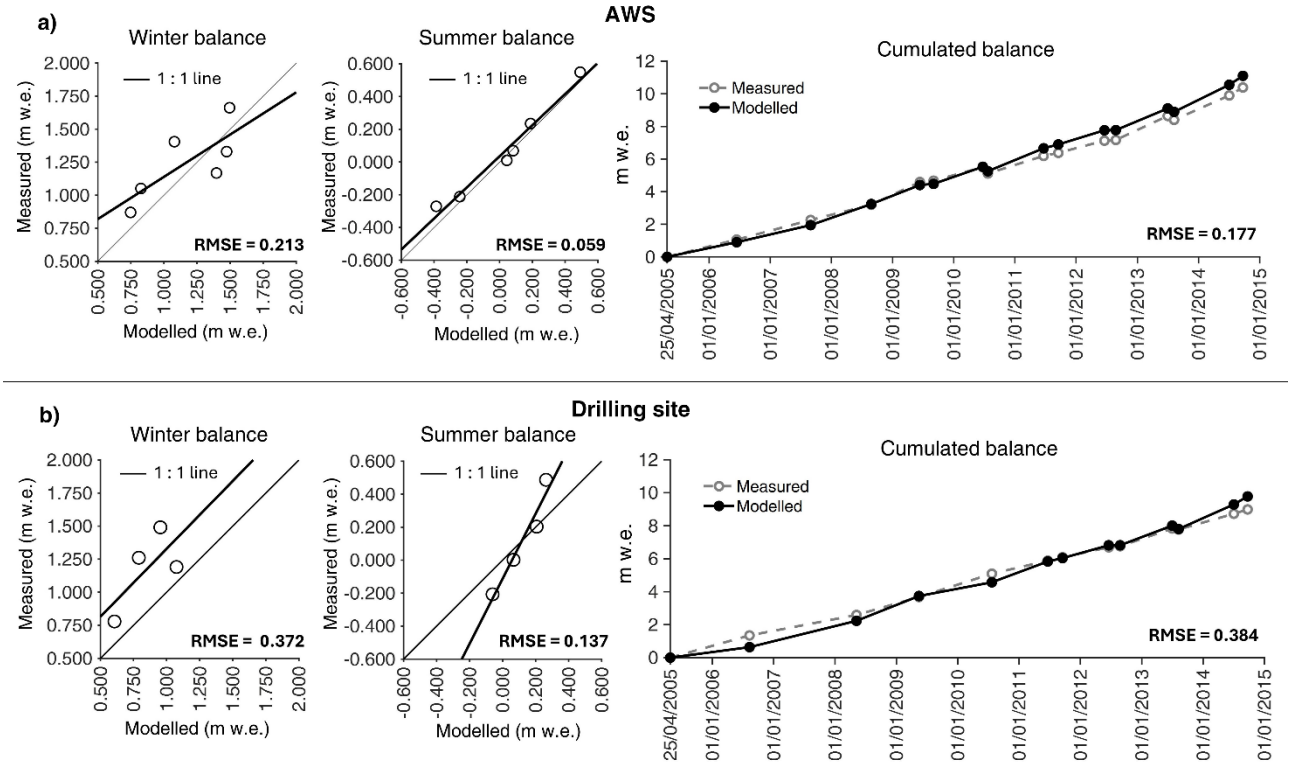


Figure 3: EISModel calibration results obtained on Mt. Ortles at a) the AWS site and b) the drilling site, for winter, summer and cumulated mass balance, in the period (2005-2014).

## 4.2 Mass balance behaviour

Based on EISModel calculations, 21.4 and 18.9 m w.e. accumulated from September 1996 to September 2014 at the AWS and ice core drilling sites, respectively (Fig. 4). Accordingly, the accumulation rate averaged 1.18 m w.e. $y^{-1}$ at the AWS site and 1.05 m w.e. $y^{-1}$ at the drilling site. The accumulation rate was smaller between 1997 and 1998 and between 2003 and 2008, and increased in the periods between 1999 and 2002 and after 2008 (Figs. 4 and 5).

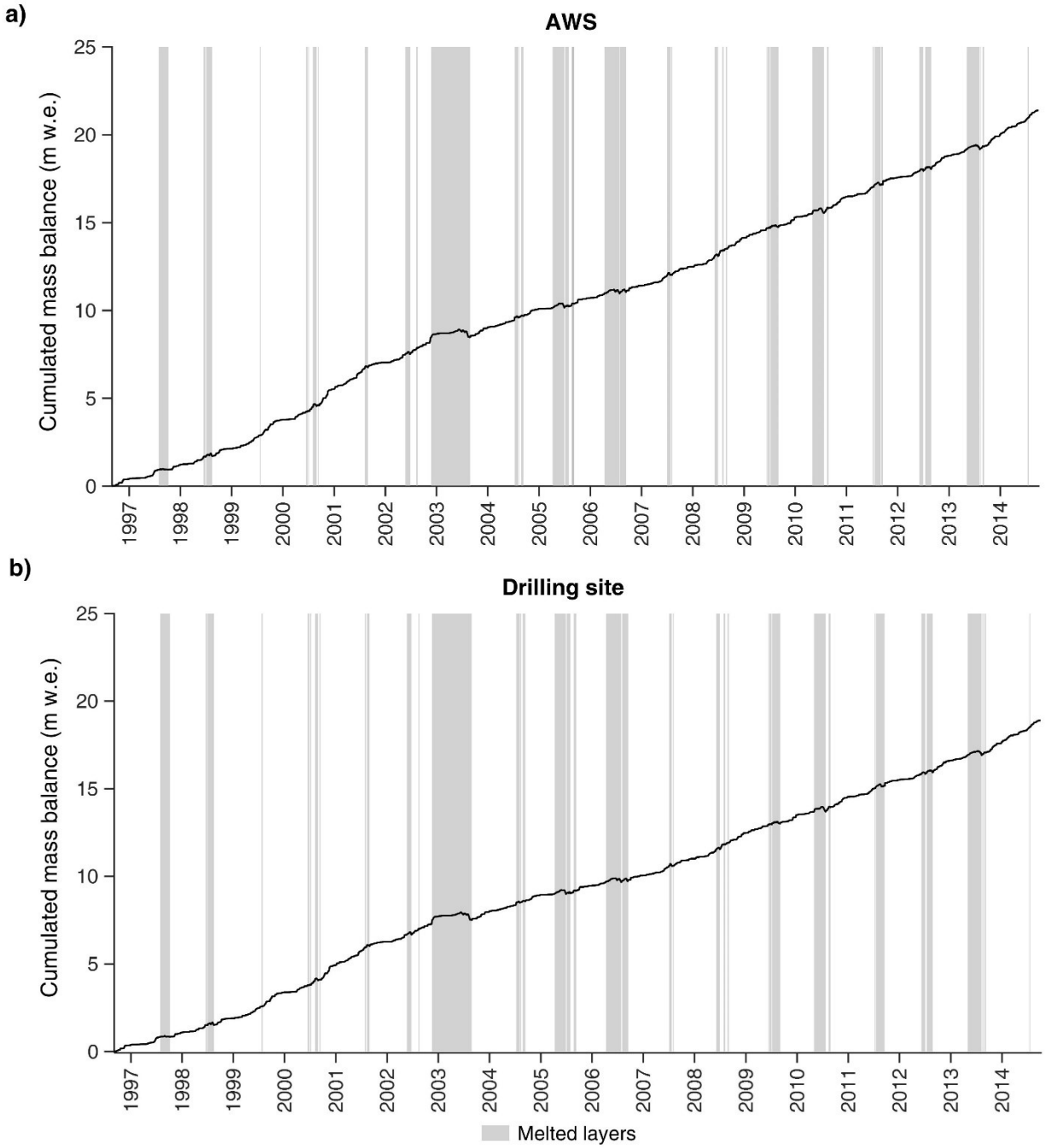


Figure 4: Cumulated mass balance modelled by EISModel at a) the AWS site and b) the drilling site. The vertical bars represent periods of snow accumulation that were removed by melt: large bars mean melting of snow accumulated over long periods (several months), whereas thin bars mean melt of snow accumulated over short periods.

The interannual variability of mass balance was remarkable at both sites (Fig. 5). The annual balance was closely correlated with the winter balance ($r = 0.80$) and slightly less correlated with the summer balance ($r = 0.78$). The summer balance was +0.25 m w.e. on average, but was close to zero in 2005, 2006 and 2013, and negative only in 2003 (-0.30 m w.e.).

253 The total melt (Fig. 5b) was also highly variable from year to year, and ranged between 0.19 m w.e. in 1999 and 0.76 m
254 w.e. in 2003. A few phases of intense and prolonged melt in 2003, 2005, 2006, 2009, 2013 and 2010 led to the removal
255 of snow layers accumulated over long periods (Fig. 4). According to EISModel calculations, the snow accumulated
256 between 17 November 2002 and 27 August 2003 (more than 9 months) was entirely melted during the 2003 European
257 heat wave. Five months of snow accumulation were removed in 2006 (from early April to early September), 4 months in
258 2005 (from early April to July), 3 months in 2013 (from May to early August), 3 months in 2009 (from June to August)
259 and 3 months in 2010 (from May to July).

260 The two years with best preservation of accumulated snow were 1999 and 2014, when melt was scarce (0.195 and 0.253
261 m w.e., respectively) and discontinuous. In these cases, melt removed only short periods of snow accumulation during
262 summer, without melting the older layers underneath and thus preserving snow accumulated during previous seasons.

263

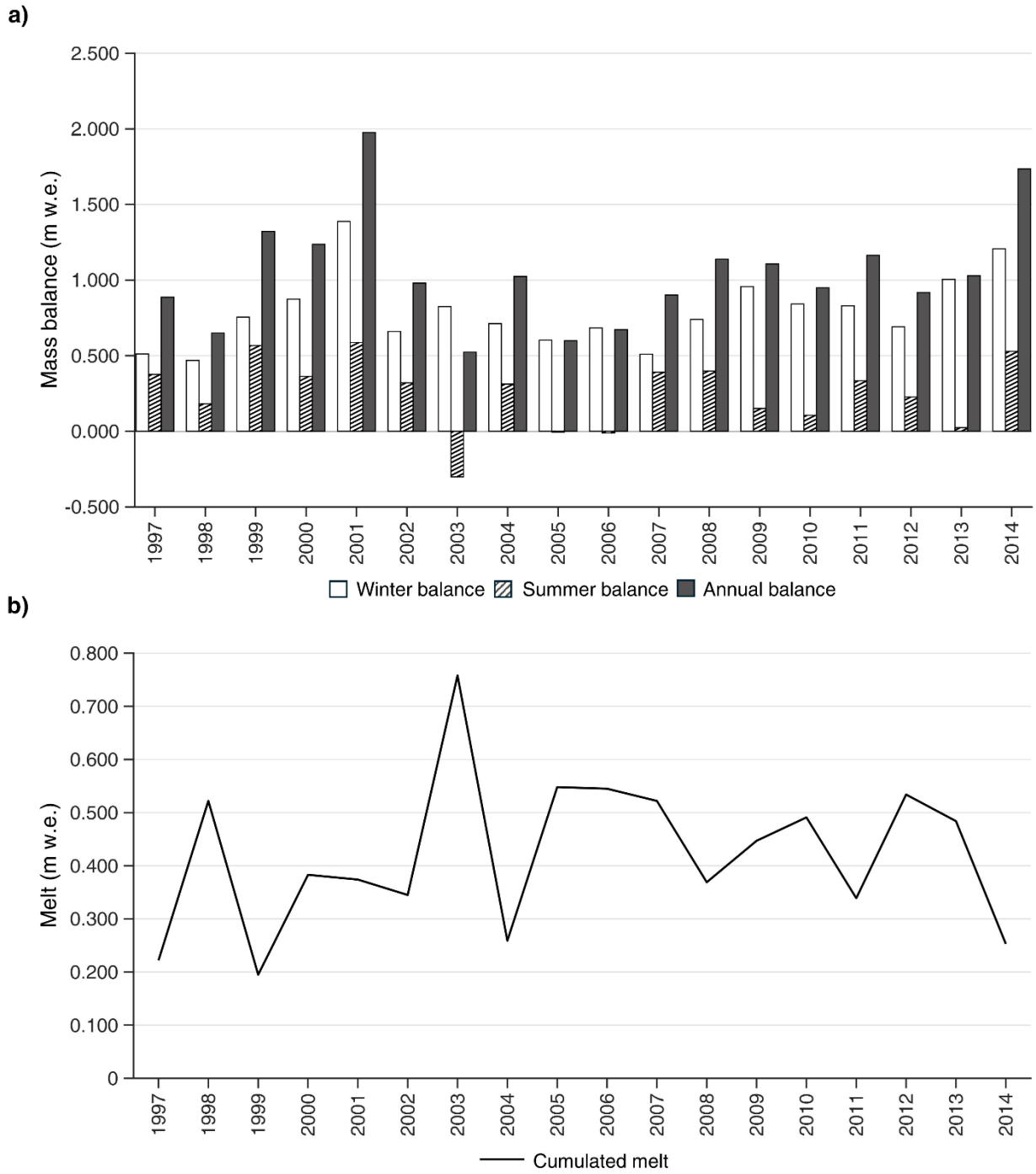


Figure 5: Interannual variability of a) seasonal and annual balance, and b) annual cumulated melt based on EISModel calculation at the Ortles drilling site.

### 4.3 The modelled pseudo proxy

In the analysed period, the pseudo proxy SLFT series calculated by EISModel shows high interannual variability in the seasonality (i.e. the difference in SLFT between winter and summer) and in the accumulation of firn layers preserving a paleoclimatic signal (Fig. 6).

According to the model, during the years 2009-2011 snow accumulation largely offset ablation in both winter and summer, preserving a marked seasonality in the pseudo proxy signal, with a good amplitude. Much less winter snow accumulated in the two years 2007 and 2008, as can be seen from the thinner grey bars in Fig. 6. This caused narrower troughs in SLFT, especially for 2007, whose trough is also higher compared to the following years. This is due to scarce snow accumulation in the coldest months of winter 2007.

In 2006, summer ablation was 30% larger than average and removed the snow deposited from April to August. Nevertheless, a large seasonal variation in SLFT is preserved thanks to snow accumulation in the coldest part of winter and in late summer. A very sharp transition between cold and warm SLFT is observable in 2006 because winter and summer layers are in direct contact. In 2005, the cold-season trough in SLFT is barely visible because snow accumulation in winter was scarce and spring snow was almost completely removed by melt.

The year 2004 shows a marked seasonality and a well-defined winter trough (comparable to that of 2006) thanks to good winter accumulation and low summer ablation (Fig. 5). The two years 2002 and 2003 look like a single year, because the exceptionally warm summer 2003 completely removed the snow accumulated in the winter season 2002-'03. The winter 2003 SLFT trough is therefore entirely missing from the record, and the November 2002 layers are in direct contact with those of late August 2003 (thin white band between the 2003 and 2004 cold-season grey bars in Fig. 6). This is important when counting annual layers and establishing a chronology in the firn core (see discussion below). Winter snow accumulation was almost absent in the hydrological year 2001-'02, causing the formation of a rather warm cold-season trough in SLFT.

High snow accumulation and low summer melt occurred in the 1999, 2000 and 2001 balance years. 2001 was a record-setting winter accumulation year in this geographic area (Armando et al., 2002), as can be seen by the width of the cold-season grey bar in Fig. 6. Summer accumulation was also the highest in the analysed period (Fig. 5). In 1999, there was high summer accumulation, combined with negligible ablation, thus making it the second highest summer balance of the analysed period.

In 1998 and especially in 1997, the seasonal variation of SLFT declines due to the very low accumulation in the coldest months (lowest winter balance of the entire series, Fig. 5) and to the removal of the 1997 summer snow layers caused by an anomalous late-summer melt event, between August and September.

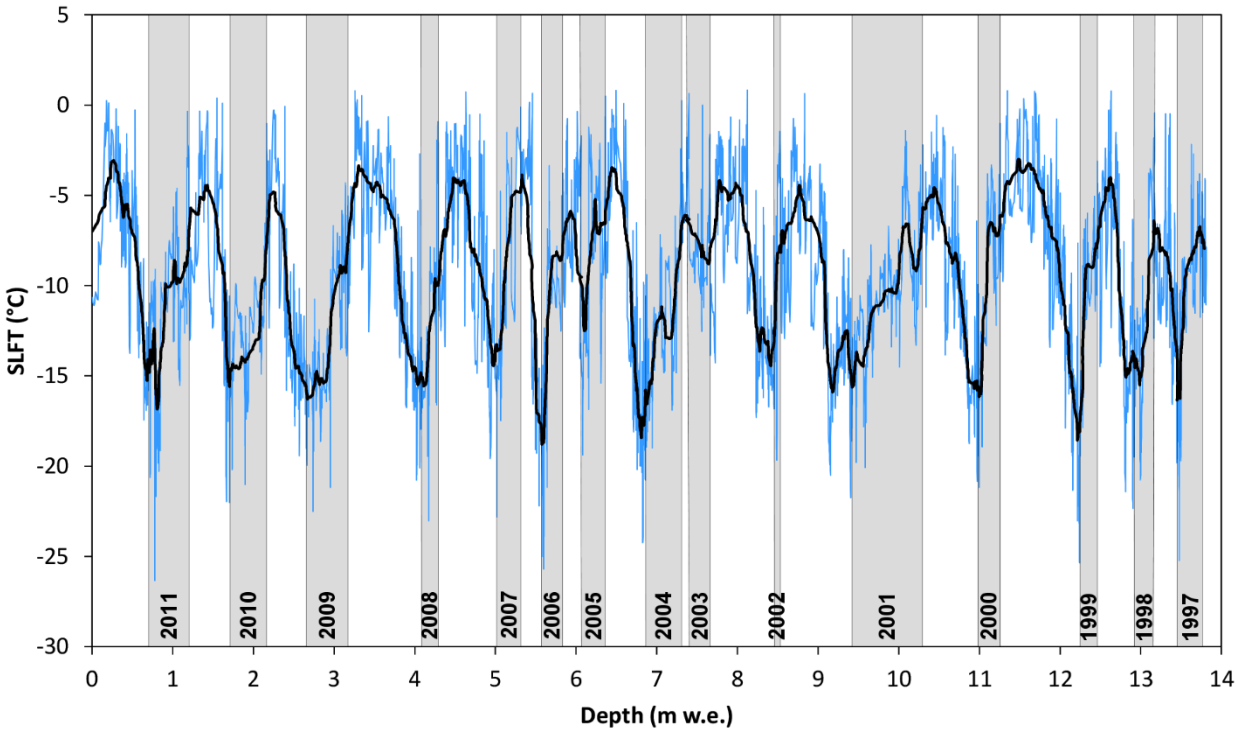


Figure 6: Snow layer formation temperature (SLFT) modelled at the drilling site by EISModel from September 1, 1996 to September 30, 2011. The black line is a 100-order centred moving average. The grey bars represent months from October to January (when pollen is not released, Fig. 7), in order to facilitate the following comparisons. The year is referred to the month of January (e.g., winter 1996-'97 is indicated as '1997').

### 4.4 Timescale based on pollen and stable isotopes

A tentative dating of the firn core extracted on Mt. Ortles was carried out based on annual layer counting based on stable isotopes and pollen measurements in the firn core (Fig. 7). We considered the depth interval from zero to 14 m w.e., the same as shown in Fig. 6. Winter layers were assigned based on troughs in the stable isotope series combined with very low/zero values in pollen concentration and PCA component scores (Section 3.2). Peaks in pollen concentration reflect the flowering season (Spring to Summer), while the lack of pollen indicates the non-flowering season (Autumn-Winter). Within each year, peaks in PC components indicate the presence of pollen types deriving from plant species blooming during spring, early summer and late summer (Festi et al., 2015 and 2017). This initial tentative timescale should represent 'routine' annual layer counting obtained using only experimental ice core data (like, for example, in Andersen et al., 2006; Takeuchi et al., 2019; Sinnl et al., 2022), independently from meteorological data or glacier mass balance observations or models.

The isotopic record is well preserved in the most recent four years (2011-2008) and is clearly smoothed by meltwater percolation before 2008, supporting the conclusions presented by Gabrielli et al. (2010). Stable isotope and pollen peaks match well within the firn layers. The pollen seasonality is well preserved for most years, except for 1999, 2006 and 2007, where the signals from spring, early summer, and late summer overlap. According to this initial tentative dating, the snow accumulation rate was larger before 2006 and smaller afterwards. When considering the layers with smoothed isotopes, there is a distinct peak that could initially be attributed to summer 2003; however, this is in clear contrast with EISModel

calculations, which indicate a complete ablation of the 2003 summer layers and removal of the associated isotopic signal (Section 4.3).

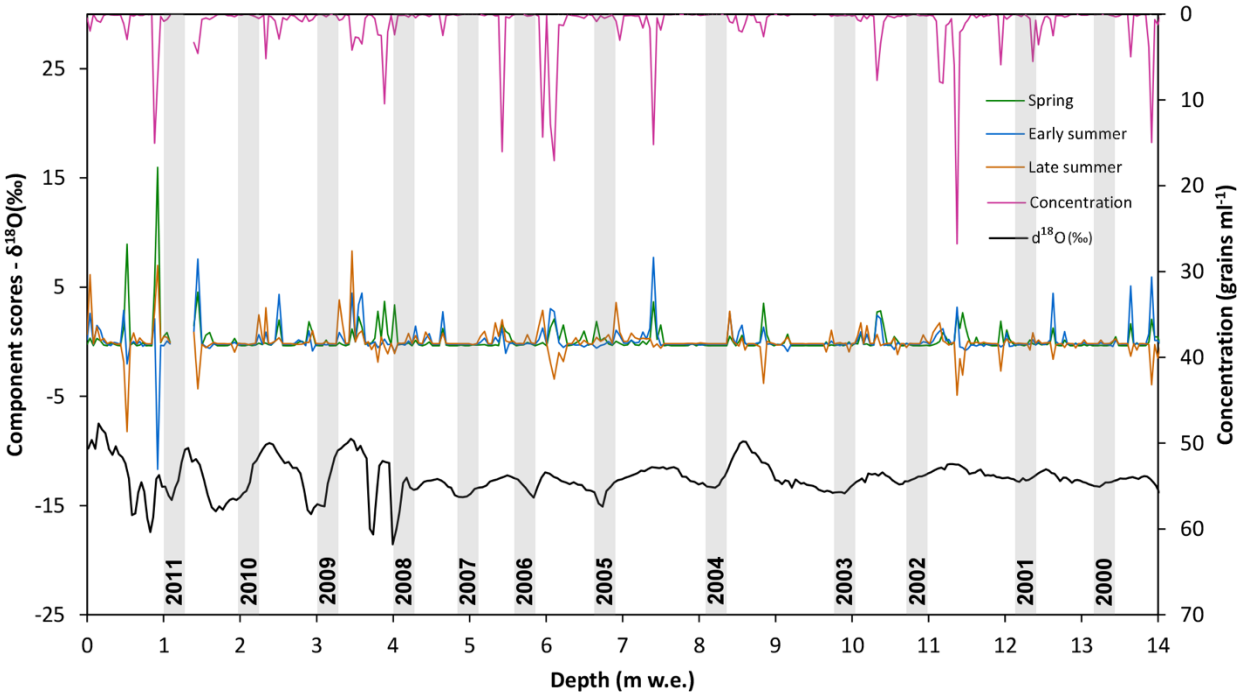


Figure 7: Concentration (right Y-axis) and principal component scores (left Y-axis) representative of spring, early summer and late summer of pollen data extracted from the Mt. Ortles core 1, compared with the $\delta^{18}O$ values (left Y-axis) determined in the same core. Grey bars represent mid-winter months (December and January) based on pollen data, and have arbitrary width. Annual layer counting is based on $\delta^{18}O$ and pollen evidence.

### 4.5 Refined dating using the modelled pseudo proxy

A refinement of the tentative timescale in Fig. 7, based on the SLFT pseudo proxy modelled by EISModel, is presented in Fig. 8. The annual layer counting from Fig. 7 matches the SLFT-based layer counting from 2011 to 2006. Below these layers, we assigned the $\delta^{18}O$ trough at ~6.8 m w.e. depth to winter 2004 (instead of 2005) and considered the ~1 m w.e. between 5.8 and 6.8 m as the result of two years of snow accumulation, 2004 and 2005. According to this interpretation, the missing trough in the winter 2005 isotopic record is due to the low winter accumulation (Fig. 5a) and to the removal of spring snow by ablation (Section 4.3, Fig. 6).

Similarly, we reinterpreted the $\delta^{18}O$ trough at ~8.2 m w.e. depth as winter 2002, whereas the winter trough of 2003 is absent in the isotopic record because those winter layers completely melted during the 2003 warm summer. The annual counting of firn layers below 2002 was consequently shifted according to these considerations, without other changes compared to Fig. 7.

This reinterpretation (Fig. 8a) presents limited chronological discrepancies compared to the SLFT pseudo proxy (Fig. 8b), without systematic under/overestimation of accumulation rates. These discrepancies would cancel each other over the depth/period considered, as can be noted from the black lines that connect Figs. 8a and 8b, whose tilt seems randomly

distributed. Interestingly the major peak in isotopes at ~8.5 m w.e. depth dates summer 2001, instead of 2003 as attributed merely on isotopes and pollen data (Section 4.4). This peak matches with the highest summer accumulation in the analysed period (Fig. 5a; Armando et al., 2001). The second highest summer accumulation year (1999) matches with the secondary peak in isotopes at ~11.5 m w.e. depth.

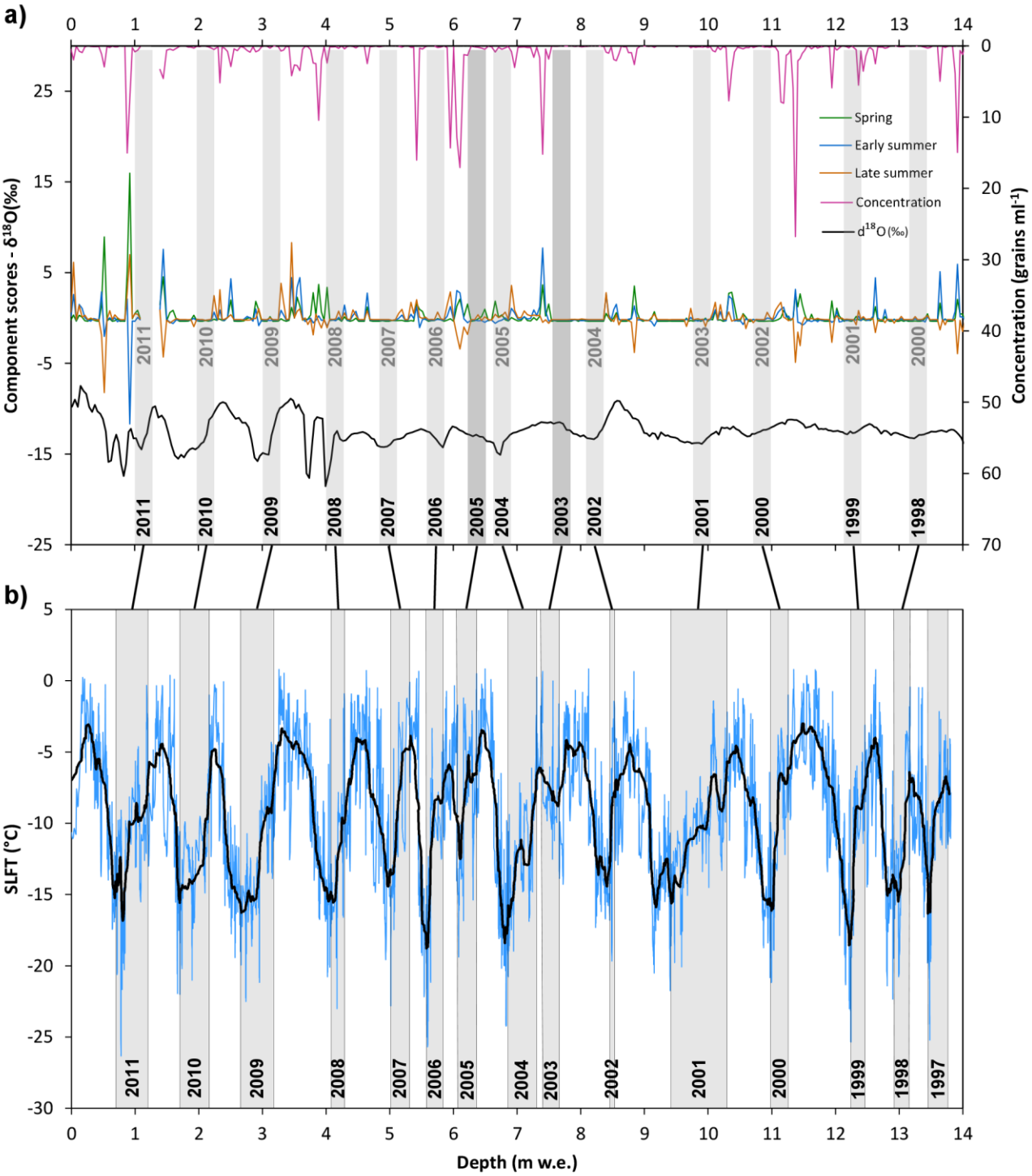


Figure 8: a) Same as Fig. 7 except annual layer counting reinterpreted based on b) snow layer formation temperature (SLFT) modelled at the drilling site using EISModel. In a) the first timescale (shown in Fig. 7) is reported with a grey

font, to ease comparison. The two darker grey bars in a) indicate winter seasons that were missed in the timescale based only on isotopes and pollen information, and added in the following using SLFT.

## 5 Discussion

The underlying assumption of our modelling approach is that the variability of local 2 m air temperature during snowfall at the drilling site (i.e. the EISModel output variable SLFT) is representative of the $\delta^{18}O$ variability in snow deposited at the same site. This is equivalent to assuming a linear relationship between 2 m air temperature and $\delta^{18}O$, whose variability is affected by other processes such as the origin and history of the water vapour in the air mass, condensation cycles, sub-cloud humidity, and preferential deposition and redistribution of snow by winds (Dansgaard, 1964; Sturm et al., 2010). Another assumption is that the original $\delta^{18}O$ variability after snow deposition was preserved on Mt. Ortles, which in realty is most likely modified by post depositional processes such as melt, sublimation, condensation, diffusion, isotopic exchange between atmospheric water vapour and snow, and percolation of melt/rainwater (Eichler et al., 2001, Steen-Larsen et al., 2014). All these effects may have caused a post-depositional increase in $\delta^{18}O$ values.

Because so many factors affect the original isotopic composition of snow and its variation through time, there are likely limitations for our approach. However, the development of EISModel and of the pseudo proxy of snow temperature formation were not intended to accurately reproduce the $\delta^{18}O$ variability measured in the ice cores retrieved on Mt. Ortles. Instead, it was designed to be a tool to improve the interpretation of paleoclimatic data preserved in snow and firn cores, particularly through more accurate firn annual layer counting. The modelling approach is based on scientific literature supporting the main assumptions that i) ice cores contain temperature information that can be extracted from stable water isotopes (e.g. Brönnimann et al., 2013; Hurley et al., 2016, Steiger et al., 2017) and ii) this temperature information and its seasonal signature are preserved (although smoothed) after limited meltwater percolation (e.g. Moser et al., 2024). However, completely melted layers cannot be represented in the retrieved stable isotope record, and the EISModel specifically accounts for that.

The EISModel is an intermediate-complexity model aiming at representing the dominant processes affecting glacier mass balance and paleoclimate proxy formation/preservation, while requiring only a few meteorological input data (precipitation and air temperature). According to Evans et al. (2013), best-compromise models for paleoclimatic applications are more complex than univariate-linear in their response to environmental forcings, without the need to capture all fine-scale processes at play in a given proxy system.

At the Mt. Ortles drilling site, the two major processes that likely influence the formation and preservation of the isotopic record are i) the seasonal distribution of precipitation/accumulation (taking into account the seasonal wind erosion) and ii) the intensity and duration of summer ablation. Both show high interannual variability (Fig. 5), which is typical of the climate of this region. Due to their importance and strong variability in time, they are explicitly modelled by EISModel to build a pseudo proxy (SFLT) that can be helpful in studying ice core records retrieved at similar sites.

EISModel does not account for the effects of meltwater percolation through snow and firn, which is highly complex and variable in space and time, depending on the thermal, stratigraphic and hydrologic structure of the subsurface (Pfeffer and Humphrey, 1998; Jennings et al., 2018; Samimi et al., 2020; Humphrey et al., 2021). Modelling water percolation should include saturation, refreezing, drainage and snow metamorphism processes. Similarly, the degradation of the isotopic record due to the meltwater infiltration is dependent on phase changes and isotopic exchange between liquid

water and the surrounding ice matrix. (Koerner et al., 1973; Lee et al., 2020). The redistribution of isotopic signatures into deeper layers causes the mixing of isotopic signatures from different seasons/years and leads to their typical smoothing in percolation-affected snow and firn layers (Koerner, 1997). The preservation of deposited isotopic signatures remains a subject of research (Moser et al., 2024), and their modifications due to percolating meltwater would require a physically-based approach to be properly modelled. Such a refinement was beyond the aims of the pseudo proxy we developed in this work.

Overall, considering the model used and the characteristics of the study area, the model's skill in reproducing observed mass balance is satisfying (Fig. 3) because the magnitude of RMSE values is comparable to the typical errors in mass balance measurements (Zemp et al., 2013). A major simplification of our model is the use of a linear relationship between accumulation and precipitation, meaning time-invariant vertical precipitation gradient and wind redistribution. This is common in glacier mass balance models of similar complexity and is unavoidable without additional in-situ direct observations of precipitation and snow redistribution.

The impact of this simplification is visible in the simulations of winter balance, which display a higher RMSE compared to summer balance (Fig. 3). However, it must be considered that uncertainty and high spatial variability also affect winter balance field measurements, not only simulations. Differences up to 0.5 m in snow depth above previous year's summer surface were measured within soundings that were just 10 m apart. This is exacerbated by the difficulty of identifying the summer surface in snow pits and snow depth soundings. However, since the RMSE does not exceed one third of the annual snow accumulation rate, we are confident in the overall model's skill to discriminate between high and low accumulation years/seasons.

Our approach share some similarities to that used by Brönnimann et al. (2013) who replicated the ice core from the Grenzgletscher (Switzerland, 4200ma.s.l.) on a sample-by-sample basis by calculating precipitation-weighted temperature (PWT) over short core intervals. However, this approach did not account for melt, whose effects are instead explicitly calculated by our glacier mass balance model. Considering the increasing air temperature, melt events are increasingly affecting high-altitude regions of temperate mountain areas, resulting in strong alterations of glacier mass balance and vertical shift of dry-snow/percolation/wet-snow zones on glaciers. Besides deterioration of paleoclimatic information contained in ice cores due to meltwater percolation, exceptional melt events can physically remove months of snow accumulation from glaciers. This is happening at increasingly high elevation in the European Alps (Baroni et al., 2023; Carrer et al., 2023) and is no longer limited to drilling sites below 4000 m a.s.l. (Huber et al., 2024). Even though current melt rates are extremely high, similar intensity of melt might have occurred also in past epochs, for example during the Holocene thermal maximum (Renssen et al., 2012; Kalis et al., 2003).

For these reasons, embedding a glacier mass balance model in proxy system models is a useful approach because of the importance of ablation, together with accumulation, in determining how the climatic signal is recorded in the ice core paleoclimatic records. Even though ablation may be assumed as negligible at an ice core drilling site at the present time under the current climate, it might have been significant in the past, particularly at glacial-interglacial time scales. Therefore, testing how melt events impact ice core records by means of glacier mass balance models embedded in proxy system models can be useful for improved dating and interpretation of these paleoclimatic archives.

The SLFT pseudo proxy clearly adds robustness to the firn core chronology, because it explicitly highlights the interannual variability of snow accumulation and ablation. Nevertheless, the interpretation of some features in the stable isotopes and pollen records remain uncertain. For example, the $\delta^{18}O$ peak at ~ 8.5 m w.e. (Figs. 7 and 8) is anomalous,

considering that the records from this section of the core were smoothed by melt water percolation. In Section 4.5 we tentatively attributed this peak to the very high summer accumulation in 2001 (Fig. 5), but there might be alternative explanations.

For instance, post-depositional effects due to the 2003 European heat wave could have caused an increase in $\delta^{18}O$ values of the snow layers re-exposed during this extreme heat event, similarly to what has been observed for post depositional changes of the isotopic composition of surface snow on the Greenland ice sheet (Steen-Larsen et al., 2014). In 2003, on Mt. Ortles, the strong percolation of melt water might have relocated pollen grains (vertical and/or lateral drainage, e.g. Ewing et al., 2014) thus explaining the relative scarcity of pollen in the 2001 and 2002 layers in Fig. 8a.

The lack of a distinct peak in this section of the SLFT series, similar to the peak at ~ 8.5 m w.e. observable in the δ18O series, might suggest that the latter depends on post-depositional effects that are not considered in the ESIModel, like sublimation, condensation, diffusion, and isotopic exchange between atmospheric water vapour and snow (Sokratov and Golubev, 2009; Steen-Larsen et al., 2014; Ebner et al., 2017; Madsen et al., 2019).

As already discussed, the SLFT pseudo proxy does not account for snow redistribution by wind, which is an important process at this high-elevation site exposed to strong winds. According to snow depth observations on Mt. Ortles and similar locations in this region (e.g., Fischer et al., 2022; Carturan et al., 2023) wind erosion strongly prevents snow accumulation in the colder winter months, between January and March. For this reason, we think that further improvements in the development of the pseudo proxy might be possible by including a simple parameterization of snow erosion and its dependence on air temperature (Li and Pomeroy, 1997; He and Ohara, 2017).

## 6 Conclusions

In this paper, we present a model that simulates the mass balance history and reconstruct the glacier stratigraphy at the Mt. Ortles ice core drilling site between 1996 and 2011. The model calculates the air temperature during the formation of snow layers (SLFT). The SLFT is used as a pseudo proxy for improved dating and interpretation of the ice core paleoclimatic archive retrieved on Mt. Ortles in 2011.

The model demonstrates good skill in reproducing the observed mass balance and proves to be useful for the interpretation of the ice core data. It is particularly valuable in detecting two major ambiguities in annual layer counting based on stable water isotopes and pollens, namely the two years 2005 and 2003, which lack a winter signal in the isotopic record. Without the model reconstruction of the local mass balance, it would not have been possible to identify and quantify these two anomalies, which stemmed from melt-induced removal of snow layers accumulated over several months or seasons.

Considering the current rate of atmospheric warming and the impact of extreme melt events (such as the warm 2003 summer in the European Alps), we suggest that modelling approaches accounting for accumulation and ablation processes can be useful for understanding how the paleoclimatic signal is formed and preserved in ice cores.

These considerations may be valid for both the current warming phase and past climatic changes. Dating and interpretation of ice core records formed during the Holocene thermal maximum, for example, may present issues similar to those highlighted in this paper. During that period and perhaps in other warm phases of the Holocene (Renssen et al., 2012), above-average summer melt, melting of large quantities of snow at the surface, and variations in snow drifting likely occurred. Model-based studies similar to the one presented in this study can provide insights into these processes and can

enable detection of these events in past climate reconstructions based on ice cores, in particular those obtained near the lower altitude limit for preserving atmospheric signals in snow and ice layers.

## Data availability

Data are available from the corresponding author upon reasonable request.

## Author contributions

LC designed the methodological approach. PG, LC, RS, GDF carried out the fieldwork. FDB and TLZ processed the meteorological data. DF and KO performed the pollen analyses. PG, GD and BS performed the isotopic analyses. FC wrote the EISModel and implemented the SLFT pseudo proxy. AI and TLZ calibrated and run the EISMODEL. LC prepared the first draft of the manuscript with contributions from PG, TLZ, AI, BS, and GD. All authors contributed to the editing of the manuscript.

## Competing interests

The contact author has declared that none of the authors has any competing interests.

## Acknowledgments

The authors are grateful to all the students, technicians and scientists who contributed to the field activities in the period from 2009 to 2016; the alpine guides of the Alpinschule of Solda; the helicopter companies Airway, Air Service Center, Star Work Sky; and the Hotel Franzenshöhe for logistical support. The authors acknowledge the editor and reviewers for their comments and suggestions.

## Financial support

The research was funded by the Italian MIUR Project (PRIN 2010-11), “Response of morphoclimatic system dynamics to global changes and related geomorphological hazards” (local and national coordinators are Giancarlo Dalla Fontana and Carlo Baroni) and was carried out within the RETURN Extended Partnership and received funding from the European Union Next-GenerationEU (National Recovery and Resilience Plan – NRRP, Mission 4, Component 2, Investment 1.3 – D.D. 1243 2/8/2022, PE0000005). The core samples were obtained as part of the Mt. Ortles Ice Core Project funded by: NSF Awards 1060115 and 1461422 with the logistic support of Ripartizione Protezione antincendi e civile of the Autonomous Province of Bolzano in collaboration with the Ripartizione Opere idrauliche e Ripartizione Foreste of the Autonomous Province of Bolzano and the Stelvio National Park. This is Ortles project publication 13 (www.ortles.org).

499 **References**


500 Adler, S., Das Klima von Tirol-Südtirol-Belluno: 1981–2010; Vergangenheit-Gegenwart-Zukunft, Zentralanstalt für
501 Meteorologie und Geodynamik; Südtirol Abteilung Brand- und Zivilschutz, Bozen, 102, 2015.

502 Andersen, K. K., Svensson, A., Johnsen, S. J., Rasmussen, S. O., Bigler, M., R¨othlisberger, R., Ruth, U., Siggaard-
503 Andersen, M. L., Peder Steffensen, J., Dahl-Jensen, D., Vinther, B. M., and Clausen, H. B.: The Greenland ice core
504 chronology 2005, 15–42 ka. Part 1: constructing the time scale, Quaternary Sci. Rev., 25, 3246–3257,
505 https://doi.org/10.1016/j.quascirev.2006.08.002, 2006.

506 Armando, E., Baroni, C., and Zanon, G.: Reports of the glaciological survey 2000. Relazioni della campagna glaciologica
507 2000, Geogr. Fis. e Din. Quat.,, 24(2), 203-261, 2001.

508 Baroni C., Bondesan, A., Carturan, L., Chiarle, M., and Scotti R.: Annual glaciological survey of Italian glaciers (2022)
509 | Campagna glaciologica annuale dei ghiacciai italiani (2022), Geogr. Fis. e Din. Quat.,, 46(1), 3-123,
510 https://doi.org/10.4454/gfdq.v46.883, 2023.

511 Bohleber, P.: Alpine Ice Cores as Climate and Environmental Archives. In P. Bohleber, Oxford Research Encyclopedia
512 of Climate Science. Oxford University Press, https://doi.org/10.1093/acrefore/9780190228620.013.743, 2019.

513 Bohleber, P., Schwikowski, M., Stocker-Waldhuber, M., Fang, L., and Fischer, A.: New glacier evidence for ice-free
514 summits during the life of the Tyrolean Iceman. Sci. Rep-UK, 10(1), 20513, https://doi.org/10.1038/s41598-020-77518-
515 9, 2020.

516 Bohleber, P., Wagenbach, D., Schöner, W., and Böhm, R.: To what extent do water isotope records from low
517 accumulation Alpine ice cores reproduce instrumental temperature series? Tellus B, 65(1), 20148,
518 https://doi.org/10.3402/tellusb.v65i0.20148, 2013.

519 Brönnimann, S., Mariani, I., Schwikowski, M., Auchmann, R., and Eichler, A.: Simulating the temperature and
520 precipitation signal in an Alpine ice core, Clim. Past, 9, 2013–2022, https://doi.org/10.5194/cp-9-2013-2013, 2013.

521 Carrer, M., Dibona, R., Prendin, A. L., and Brunetti, M.: Recent waning snowpack in the Alps is unprecedented in the
522 last six centuries, Nat. Clim. Chang., 13, 155–160, https://doi.org/10.1038/s41558-022-01575-3, 2023.

523 Carturan, L., Cazorzi, F., and Dalla Fontana, G.: Distributed mass-balance modelling on two neighbouring glaciers in
524 Ortles-Cevedale, Italy, from 2004 to 2009, J. Glaciol., 58(209), 467-486, https://doi.org/10.3189/2012JoG11J111, 2012a.

525 Carturan L., Dalla Fontana, G., and Borga, M.: Estimation of winter precipitation in a high-altitude catchment of the
526 Eastern Italian Alps: validation by means of glacier mass balance observations, Geogr. Fis. e Din. Quat., 35, 37-48,
527 https://doi.org/10.4461/GFDQ.2012.35.4, 2012b.

528 Carturan, L., De Blasi, F., Dinale, R., Dragà, G., Gabrielli, P., Mair, V., Seppi, R., Tonidandel, D., Zanoner, T., Zendrini,
529 T. L., and Dalla Fontana, G.: Modern air, englacial and permafrost temperatures at high altitude on Mt Ortles
530 (3905 m a.s.l.), in the eastern European Alps, Earth Syst. Sci. Data, 15, 4661–4688, https://doi.org/10.5194/essd-15-4661-
531 2023, 2023.

532 Cazorzi, F., and Dalla Fontana, G.: Snowmelt modelling by combining air temperature and a distributed radiation index.
533 J. Hydrol., 181(1–4), 169–187, https://doi.org/10.1016/0022-1694(95)02913-3, 1996.

Dansgaard, W.: Stable isotopes in precipitation, Tellus, XVI, 436–468, 1964.

Dietermann, N., and Weiler, M.: Spatial distribution of stable water isotopes in alpine snow cover, Hydrol. Earth. Syst. Sc., 17(7), 2657–2668, https://doi.org/10.5194/hess-17-2657-2013, 2013.

Ebner, P. P., Steen-Larsen, H., Stenni, B., Schneebeli, M., and Steinfeld, A.: Experimental Observation of Transient δ18O Interaction between Snow and Advective Airflow under Various Temperature Gradient Conditions, The Cryosphere, 11, 1733–1743, https://doi.org/10.5194/tc-11-1733-2017, 2017.

Eichler, A., Schwikowski, M., Gäggeler, H. W., Furrer, V., Synal, H.-A., Beer, J., Saurer, M., and Funk, M.: Glaciochemical dating of an ice core from the upper Grenzgletscher (4200ma.s.l.), J. Glaciol., 46, 507–515, https://doi.org/10.3189/172756500781833098, 2000.

Eichler, A., Schwikowski, M., and Gäggeler, H. W.: Meltwater-induced relocation of chemical species in Alpine firn, Tellus B, 53, 192–203, https://doi.org/10.3402/tellusb.v53i2.16575, 2001.

Ekaykin, A. A. and Lipenkov, V. Y.: Formation of the ice core isotopic composition, Physics of ice core records, Low Temp. Sci., 68, 299–314, 2009.

Erdtman, G.: The acetolysis method. A revised description. Svensk Bot. Tidskr., 54, 561–569, 1960.

Evans, M. N., Tolwinski-Ward, S. E., Thompson, D. M., and Anchukaitis, K. J.: Applications of proxy system modeling in high resolution paleoclimatology, Quaternary Sci. Rev., 76, 16-28, https://doi.org/10.1016/j.quascirev.2013.05.024, 2013.

Ewing, M. E., Reese, C. A., and Nolan, M. A.: The potential effects of percolating snowmelt on palynological records from firn and glacier ice. J. Glaciol., 60(222), 661-669, doi:10.3189/2014JoG13J158, 2014.

Faegri, K., Iversen, J., Kaland, P. E., and Krzywinski, K.: Bestimmungsschlüssel für die nordwesteuropäische Pollenflora. Gustav Fischer, Jena, 1993.

Festi, D., Carturan, L., Kofler, W., dalla Fontana, G., de Blasi, F., Cazorzi, F., Bucher, E., Mair, V., Gabrielli, P., and Oeggl, K.: Linking pollen deposition and snow accumulation on the Alto dell'Ortles glacier (South Tyrol, Italy) for sub-seasonal dating of a firn temperate core, The Cryosphere, 11, 937–948, https://doi.org/10.5194/tc-11-937-2017, 2017.

Festi, D., Kofler, W., Bucher, E., Carturan, L., Mair, V., Gabrielli, P., and Oeggl, K.: A novel pollen-based method to detect seasonality in ice cores: a case study from the Ortles glacier, South Tyrol, Italy, J. Glaciol., 61, 815–824, doi:10.3189/2015JoG14J236, 2015.

Festi, D., Schwikowski, M., Maggi, V., Oeggl, K., and Jenk, T. M.: Significant mass loss in the accumulation area of the Adamello glacier indicated by the chronology of a 46m ice core, The Cryosphere, 15, 4135–4143, https://doi.org/10.5194/tc-15-4135-2021, 2021.

Fischer, A., Stocker-Waldhuber, M., Frey, M., and Bohleber, P.: Contemporary mass balance on a cold Eastern Alpine ice cap as a potential link to the Holocene climate. Sci Rep 12, 1331, https://doi.org/10.1038/s41598-021-04699-2, 2022.

566 Gabrielli, P., Carturan, L., Gabrieli, J., Dinale, R., Krainer, K., Hausmann, H., Davis, M., Zagorodnov, V., Seppi, R.,
567 Barbante, C., Fontana, G. D., and Thompson, L. G.: Atmospheric warming threatens the untapped glacial archive of
568 Ortles mountain, South Tyrol, J. Glaciol,, 56, 843–853, https://doi.org/10.3189/002214310794457263, 2010.

569 Gabrielli, P., Barbante, C., Bertagna, G., Bertó, M., Binder, D., Carton, A., Carturan, L., Cazorzi, F., Cozzi, G., Dalla
570 Fontana, G., Davis, M., De Blasi, F., Dinale, R., Dragà, G., Dreossi, G., Festi, D., Frezzotti, M., Gabrieli, J., Galos, S. P.,
571 Ginot, P., Heidenwolf, P., Jenk, T. M., Kehrwald, N., Kenny, D., Magand, O., Mair, V., Mikhalenko, V., Lin, P. N.,
572 Oeggl, K., Piffer, G., Rinaldi, M., Schotterer, U., Schwikowski, M., Seppi, R., Spolaor, A., Stenni, B., Tonidandel, D.,
573 Uglietti, C., Zagorodnov, V., Zanoner, T., and Zennaro, P.: Age of the Mt. Ortles ice cores, the Tyrolean Iceman and
574 glaciation of the highest summit of South Tyrol since the Northern Hemisphere Climatic Optimum, The Cryosphere, 10,
575 2779–2797, doi:10.5194/tc-10-2779-2016, 2016.

576 Gabrielli, P., Barbante, C., Carturan, L., Cozzi, G., Dalla Fontana, G., Dinale, R., Draga, G., Gabrieli, J., Kehrwald, N.,
577 Mair, V., Mikhalenko, V. N., Piffer, G., Rinaldi, M., Seppi, R., Spolaor, A., Thompson, L. G., and Tonidandel, D.:
578 Discovery of cold ice in a new drilling site in the Eastern European Alps, Geogr. Fis. Dinam. Quat., 35, 101–105,
579 doi:10.4461/GFDQ.2012.35.10, 2012

580 García-Herrera, R., Díaz, J., Trigo, R. M., Luterbacher, J., and Fischer, E. M.: A Review of the European Summer Heat
581 Wave of 2003, Crit. Rev. Env. Sci. Tec., 40(4), 267–306. https://doi.org/10.1080/10643380802238137, 2010.

582 Haeberli, W., and Alean, J.: Temperature and accumulation of high altitude firn in the Alps, Ann. Glaciol., 6, 161-163,
583 https://doi.org/10.3189/1985AoG6-1-161-163, 1985.

584 Hashimoto, S., Zhou, S., Nakawo, M., Shimizu, M., and Ishikawa, N.: Temporal isotope changes in wet snow layers in
585 association with mass exchange between snow particles and liquid water in between the particles, Ann. Glaciol., 40, 128–
586 132, https://doi.org/10.3189/172756405781813492, 2005.

587 Humphrey, N. F., Harper, J. T., and Meierbachtol, T. W.: Physical limits to meltwater penetration in firn, J. Glaciol., 67,
588 952–960, https://doi.org/10.1017/jog.2021.44, 2021.

589 Hurley, J. V., M. Vuille, and D. R. Hardy (2016), Forward modeling of $\delta$18O in Andean ice cores, Geophys. Res. Lett.,
590 43, 8178–8188, https://doi.org/10.1002/2016GL070150, 2005.

591 He, S., and Ohara, N.: A new formula for estimating the threshold wind speed for snow movement, J. Adv. Model. Earth.
592 Sy., 9, 2514–2525. https://doi.org/10.1002/2017MS000982, 2017.

593 Horita, J., Ueda, A., Mizukami, K., and Takatori, I.: Automatic δD and δ18O analyses of multi-water samples using H2–
594 and CO2–water equilibration methods with a common equilibration set-up, Appl. Radiat. Isot., 40, 801–805,
595 https://doi.org/10.1016/0883-2889(89)90100-7, 1989.

596 Huber, C. J., Eichler, A., Mattea, E., Brütsch, S., Jenk, T. M., Gabrieli, J., Barbante, C., and Schwikowski, M.: High-
597 altitude glacier archives lost due to climate change-related melting, Nat. Geosci., 17(2), 110–113.
598 https://doi.org/10.1038/s41561-023-01366-1, 2024.

599 Hurley, J. V., Vuille, M., and Hardy, D. R.: Forward modeling of $\delta$18O in Andean ice cores, Geophys. Res. Lett., 43,
600 8178–8188, https://doi.org/10.1002/2016GL070150, 2016.

Jennings, K. S., Kittel, T. G. F., and Molotch, N. P.: Observations and simulations of the seasonal evolution of snowpack cold content and its relation to snowmelt and the snowpack energy budget, The Cryosphere, 12, 1595–1614, https://doi.org/10.5194/tc-12-1595-2018, 2018.

Kalis, A. J., Merkt, J., and Wunderlich, J.: Environmental changes during the Holocene climatic optimum in central Europe-human impact and natural causes. Quat. Sci. Rev., 22(1), 33-79, https://doi.org/10.1016/S0277-3791(02)00181-6, 2003.

Koerner, R. M.: Some comments on climatic reconstructions from ice cores drilled in areas of high melt, J. Glaciol., 43, 90–97, https://doi.org/10.3189/S0022143000002847, 1997.

Koerner, R. M., Paterson, W. S. B., and Krouse, H. R.: $\delta^{18}O$ Profile in Ice formed between the Equilibrium and Firn Lines, Nature Physical Science, 245, 137–140, https://doi.org/10.1038/physci245137a0, 1973.

Laepple, T., Münch, T., Casado, M., Hoerhold, M., Landais, A., and Kipfstuhl, S.: On the similarity and apparent cycles of isotopic variations in East Antarctic snow pits, The Cryosphere, 12, 169–187, https://doi.org/10.5194/tc-12-169-2018, 2018.

Lee, J.: A numerical study of isotopic evolution of a seasonal snowpack and its meltwater by melting rates, Geosci. J., 18(4), 503–510. https://doi.org/10.1007/s12303-014-0019-5, 2014.

Lee, J., Hur, S. Do, Lim, H. S., and Jung, H.: Isotopic characteristics of snow and its meltwater over the Barton Peninsula, Antarctica, Cold. Reg. Sci. Technol., 173, 102997, https://doi.org/10.1016/j.coldregions.2020.102997, 2020.

Li, L., and J. W. Pomeroy.: Estimates of Threshold Wind Speeds for Snow Transport Using eteorological Data, J. Appl. Meteor. Climatol., 36, 205–213, https://doi.org/10.1175/1520-0450(1997)036<0205:EOTWSF>2.0.CO;2, 1997.

Madsen, M. V., Steen-Larsen, H. C., Hörhold, M., Box, J., Berben, S. M. P., Capron, E., Faber, A. K., Hubbard, A., Jensen, M. F., Jones, T. R., Kipfstuhl, S., Koldtoft, I., Pillar, H. R., Vaughn, B. H., Vladimirova, D., and Dahl-Jensen, D.: Evidence of isotopic fractionation during vapor exchange between the atmosphere and the snow surface in Greenland, J. Geophys. Res. Atmospheres, 124, 2932–2945, https://doi.org/10.1029/2018JD029619, 2019.

Moran, T., Marshall, S. J., and Sharp, M. J.: Isotope thermometry in melt-affected ice cores: ISOTOPE THERMOMETRY. J. Geophys. Res.-Earth, 116(F2), https://doi.org/10.1029/2010JF001738, 2011.

Moser, D. E., Thomas, E. R., Nehrbass-Ahles, C., Eichler, A., and Wolff, E.: Review article: Melt-affected ice cores for polar research in a warming world, The Cryosphere, 18, 2691–2718, https://doi.org/10.5194/tc-18-2691-2024, 2024.

Nakazawa, F., Fujita, K., Takeuchi, N., Fujiki, T., Uetake, J., Aizen, V., and Nakawo, M.: Dating of seasonal snow/firn accumulation layers using pollen analysis, J. Glaciol., 51(174), 483–490, https://doi.org/10.3189/172756505781829179, 2005.

Neff, P. D., Steig, E. J., Clark, D. H., McConnell, J. R., Pettit, E. C., and Menounos, B.: Ice-core net snow accumulation and seasonal snow chemistry at a temperate-glacier site: Mount Waddington, southwest British Columbia, Canada., J. Glaciol., *58*(212), 1165–1175, https://doi.org/10.3189/2012JoG12J078, 2012.

Nye, J. F.: Correction factor for accumulation measured by the thickness of the annual layers in an ice sheet, J. Glaciol., 4, 785–788, https://doi.org/10.3189/S0022143000028367, 1963.

Okazaki, A. and Yoshimura, K.: Global evaluation of proxy system models for stable water isotopes with realistic atmospheric forcing, J. Geophys. Res.-Atmos., 124, 8972–8993, https://doi.org/10.1029/2018JD029463, 2019.

Pavlova, P. A., Jenk, T. M., Schmid, P., Bogdal, C., Steinlin, C., and Schwikowski, M.: Polychlorinated Biphenyls in a Temperate Alpine Glacier: 1. Effect of Percolating Meltwater on their Distribution in Glacier Ice, Environ. Sci. Technol., 49, 14085–14091, https://doi.org/10.1021/acs.est.5b03303, 2015.

Penna, D., Stenni, B., Sanda, M., Wrede, S., Bogaard, T.A., Michelini, M., Fischer, B.M.C., Gobbi, A., Mantese, N., Zuecco, G., Borga, M., Bonazza, M., Sobotkova, M., Cejkova, B., and Wassenaar, L.I.: Technical note: Evaluation of between-sample memory effects in the analysis of δ2H and δ18O of water samples measured by laser spectroscopes, Hydrol. Earth Syst. Sci. 16, 3925–3933, https://doi.org/10.5194/hess-16-3925-2012, 2012.

Pfeffer, W. T. and Humphrey, N. F.: Formation of ice layers by infiltration and refreezing of meltwater, Ann. Glaciol., 26, 83–91, https://doi.org/10.3189/1998aog26-1-83-91, 1998.

Renssen, H., Seppä, H., Crosta, X., Goosse, H., and Roche, D. M.: Global characterization of the Holocene thermal maximum, Quat. Sci. Rev., 48, 7-19, https://doi.org/10.1016/j.quascirev.2012.05.022, 2012.

Sinnl, G., Winstrup, M., Erhardt, T., Cook, E., Jensen, C. M., Svensson, A., Vinther, B. M., Muscheler, R., and Rasmussen, S. O.: A multi-ice-core, annual-layer-counted Greenland ice-core chronology for the last 3800 years: GICC21, Clim. Past, 18, 1125–1150, https://doi.org/10.5194/cp-18-1125-2022, 2022.

Samimi, S., Marshall, S. J., and MacFerrin, M.: Meltwater Penetration Through Temperate Ice Layers in the Percolation Zone at DYE-2, Greenland Ice Sheet, Geophys. Res. Lett., 47, e2020GL089211, https://doi.org/10.1029/2020GL089211, 2020.

Sokratov, S.A., and Golubev, V.N.: Snow isotopic content change by sublimation, J. Glaciol., 55, 823–828, https://doi.org/10.3189/002214309790152456, 2009.

Steen-Larsen, H. C., Masson-Delmotte, V., Hirabayashi, M., Winkler, R., Satow, K., Prié, F., Bayou, N., Brun, E., Cuffey, K. M., Dahl-Jensen, D., Dumont, M., Guillevic, M., Kipfstuhl, S., Landais, A., Popp, T., Risi, C., Steffen, K., Stenni, B., and Sveinbjörnsdottír, A. E.: What controls the isotopic composition of Greenland surface snow?, Clim. Past, *10*(1), 377–392, https://doi.org/10.5194/cp-10-377-2014, 2014.

Steiger, N. J., Steig, E. J., Dee, S. G., Roe, G. H., and Hakim, G. J.: Climate reconstruction using data assimilation of water isotope ratios from ice cores, J. Geophys. Res. Atmospheres, 122, 1545–1568, https://doi.org/10.1002/2016JD026011, 2017.

Sturm, C., Zhang, Q., and Noone, D.: An introduction to stable water isotopes in climate models: benefits of forward proxy modelling for paleoclimatology, Clim. Past, 6(1), 115-129, https://doi.org/10.5194/cp-6-115-2010, 2010.

Takeuchi, N., Sera, S., Fujita, K., Aizen, V. B., and Kubota, J.: Annual layer counting using pollen grains of the Grigoriev ice core from the Tien Shan Mountains, central Asia, Arct. Antarct. Alp. Res., 51, 299–312, https://doi.org/10.1080/15230430.2019.1638202, 2019.

669 Thompson, L. G., Davis, M. E., Mosley-Thompson, E., Porter, S. E., Corrales, G. V., Shuman, C. A., and Tucker, C. J.:
670 The impacts of warming on rapidly retreating high-altitude, low-latitude glaciers and ice core-derived climate records,
671 Global Planet. Change, 203, 103538, https://doi.org/10.1016/j.gloplacha.2021.103538, 2021.

672 Thompson, L. G., Mosley-Thompson, E., Davis, M. E., and Brecher, H. H.: Tropical glaciers, recorders and indicators of
673 climate change, are disappearing globally, Ann. Glaciol., 52(59), 23–34, https://doi.org/10.3189/172756411799096231,
674 2011.

675 Unnikrishna, P. V., McDonnell, J. J., and Kendall, C.: Isotope variations in a Sierra Nevada snowpack and their relation
676 to meltwater, J. Hydrol., 260(1–4), 38–57, https://doi.org/10.1016/S0022-1694(01)00596-0, 2002.

677 Zemp, M., Thibert, E., Huss, M., Stumm, D., Rolstad Denby, C., Nuth, C., Nussbaumer, S. U., Moholdt, G., Mercer, A.,
678 Mayer, C., Joerg, P. C., Jansson, P., Hynek, B., Fischer, A., Escher-Vetter, H., Elvehøy, H., and Andreassen, L. M.:
679 Reanalysing glacier mass balance measurement series, The Cryosphere, 7, 1227–1245, https://doi.org/10.5194/tc-7-1227-
680 2013, 2013.